Electronic Supplementary Information for:

Polymer solution structure and dynamics within pores of hexagonally close-packed nanoparticles†

Christian M. Heil[1], Arthi Jayaraman[1,2,*]

[1]Department of Chemical and Biomolecular Engineering, 150 Academy St., University of Delaware, Newark, DE 19716. United States of America

[2]Department of Materials Science and Engineering, 201 DuPont Hall, University of Delaware, Newark, DE 19716. United States of America

*Corresponding author arthij@udel.edu

†Electronic supplementary information (ESI) available.

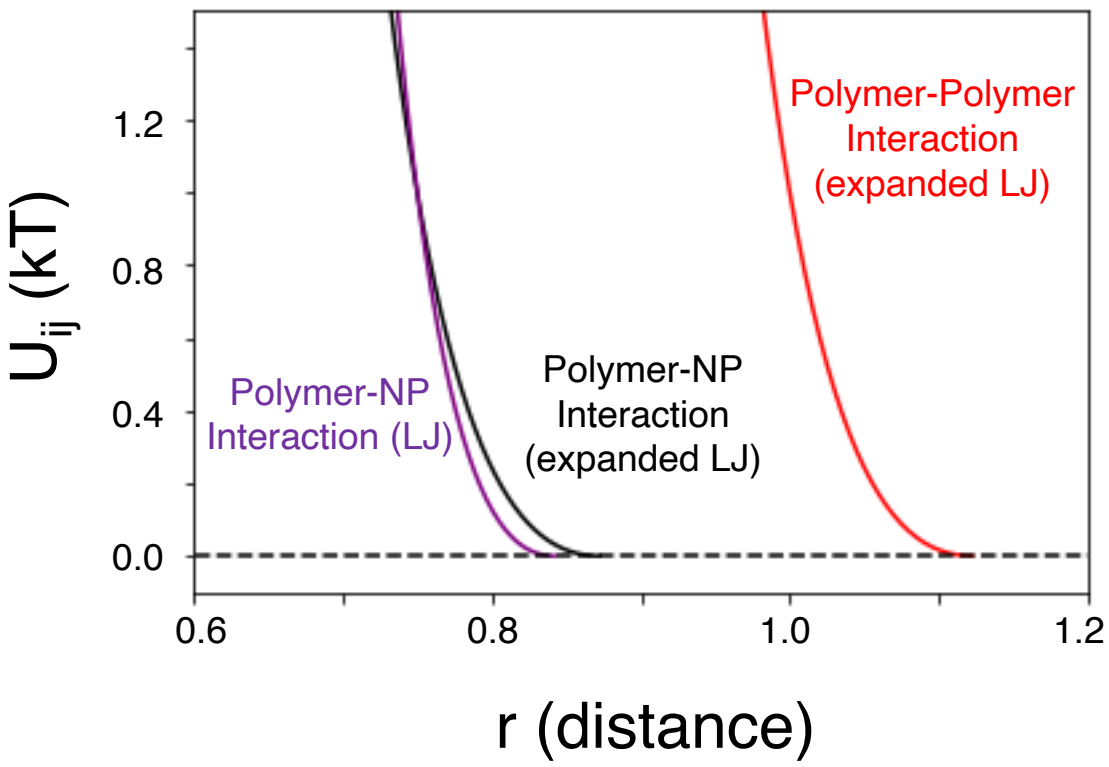

***Figure S1**: Visualization of expanded LJ potential and the traditional LJ potential. The polymer-nanoparticle used in this work is the expanded LJ interaction shown in black line; for comparison the purple line is the traditional LJ potential (set $\varepsilon_{ij} = 1.0$, $\sigma_{ij} = 0.75$ d, and r_{cut} to $2^{1/6}\sigma_{ij}$). Showing the polymer-polymer interaction (purely repulsive) for reference in red to illustrate that the 'hardness' or potential shape for polymer-polymer interaction is the same as the polymer-nanoparticle interaction (black line).*

I. Tetrahedral and octahedral pore information

For a nanoparticle-based hexagonally close-packed (HCP) crystal, the two types of pores are tetrahedral and octahedral. **Figure S2** shows how each of the pores appear in a perfect HCP crystal (top) and the simulation box used for the individual tetrahedral and octahedral pores in the main text Section III (bottom). **Table S1** provides the tetrahedral and octahedral pore radii for the largest sphere that can be placed in the pore without touching the neighboring nanoparticles based on the pore geometry.[1]

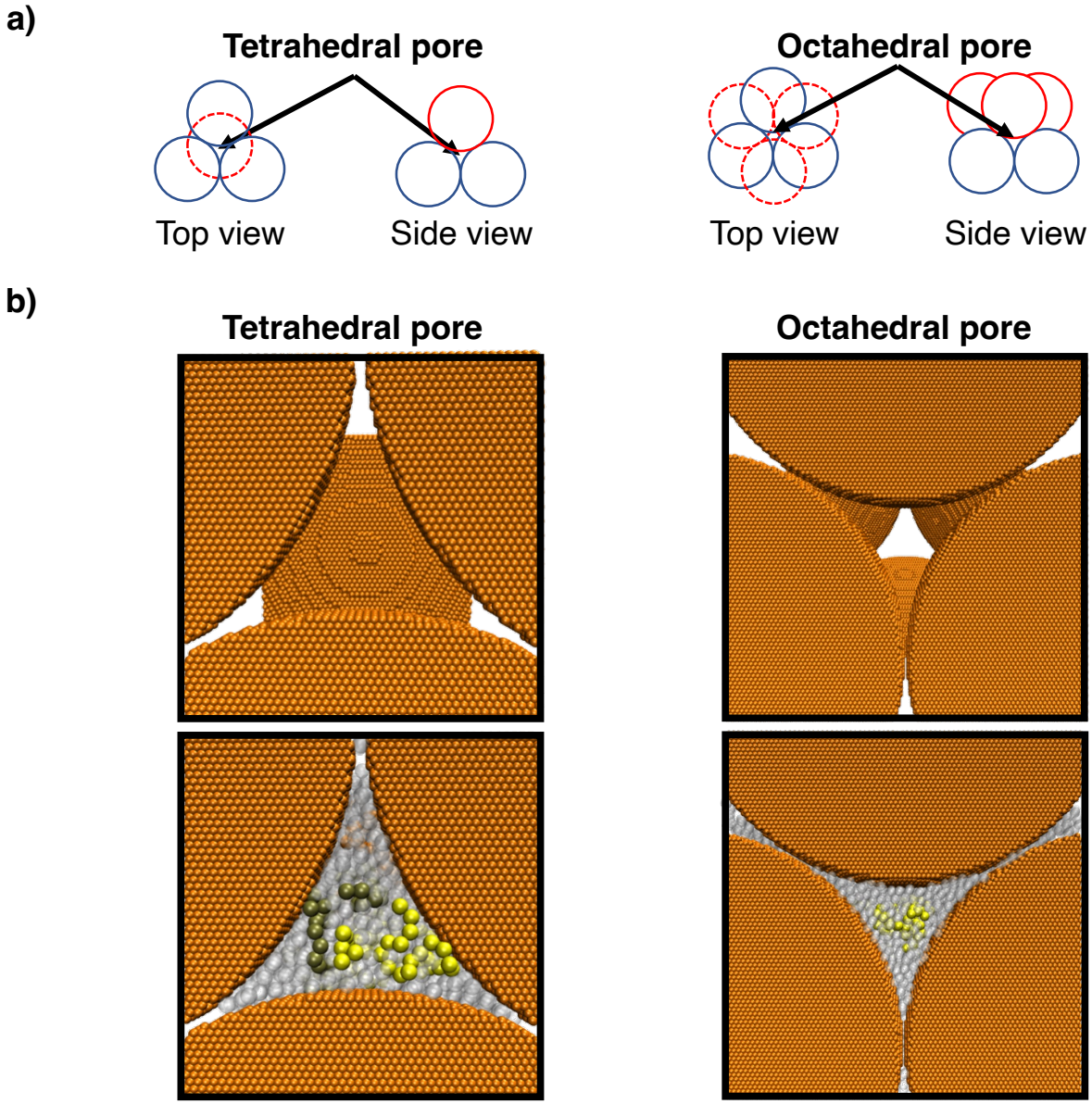

***Figure S2**: Visualization of the tetrahedral and octahedral pores found in an HCP crystal. a) provides a circle-based representation of the tetrahedral and octahedral pores with nanoparticles in different z planes marked in either blue or red. b) visualization of tetrahedral and octahedral pores as simulated in this work. The top row shows just the nanoparticles to illustrate the pore,*

and the bottom row includes the polymer (each polymer colored separately) and solvent (gray transparent spheres).

***Table S1**: Tetrahedral and octahedral pore radii*[1]

Pore type	Pore radius (percent of NP radius)	Pore radius (*d*)
Tetrahedral	~22.5%	5.625
Octahedral	~41.4%	10.35

II. Validation of bulk polymer characteristics from our simulations

We validate that the model and simulation method used in this study reproduce key polymer structural (R_g) and dynamical (polymer relaxation) scaling with polymer length and polymer concentration.[2-5] For a dilute solution, $\langle R_g^2 \rangle$ is given by:

$$\langle R_g^2 \rangle = \langle R_{g0}^2 \rangle = N^{2\nu} \quad \text{(S1)}$$

with N defined here as the number of beads in the polymer chain and ν the scaling exponent. For a good solvent (system of interest for our study), ν is expected to be ~0.6.[2-5] **ESI Figure S3a** shows the $\langle R_g^2 \rangle$ from the 1%v dilute concentration for all polymer lengths considered. Because Equation S1 is only valid for sufficiently long polymer chains, we obtain ν = 0.61 by fitting the N = 114 and N = 228 systems which is in good agreement with expectations.[2-5]

As the polymer concentration increases, the $\langle R_g^2 \rangle$ scaling with polymer concentration is given by:

$$\langle R_g^2 \rangle = \langle R_{g0}^2 \rangle \left(\frac{c}{c^*}\right)^{(2\nu-1)/(1-3\nu)} \quad \text{(S2)}$$

with c as the polymer concentration and c^* as the overlap concentration as previously defined in the manuscript. **ESI Figure S3b** shows the $\langle R_g^2 \rangle$ for the N = 114 and N = 228 systems as the polymer concentration increases causing a shift from the dilute to semi-dilute regime. The black line is Equation S2 to illustrate the change in $\langle R_g^2 \rangle$ scaling with polymer concentration with ν set to 0.61 as found above.

Finally, we demonstrate how the longest polymer relaxation time τ_r scale with polymer length and concentration (**ESI Figure S3c and S3d**). The polymer relaxation time is calculated from the polymer chain end-to-end vector autocorrelation function (Equation 3 in the manuscript). The longest polymer relaxation time is obtained by fitting an exponential decay function to the autocorrelation function to extract the relaxation time τ_r. In dilute conditions, the relaxation time should scale with polymer chain length N according to[5, 6]

$$\tau_r = N^{3\nu} \quad \text{(S3)}$$

For semi-dilute polymer solutions in the unentangled regime, the polymer relaxation time should scale with polymer concentration as

$$\tau_r = \tau_{r0} \left(\frac{c}{c^*}\right)^{(2-3\nu)/(3\nu-1)} \quad \text{(S4)}$$

For semi-dilute polymer solutions in the entangled regime, the polymer relaxation time scales as

$$\tau_r = \tau_{r0} \left(\frac{c}{c^*}\right)^{(3-3\nu)/(3\nu-1)} \quad \text{(S5)}$$

For the polymer lengths and concentrations studied in this work, the polymers are in the unentangled regime. The relaxation scaling in Equation S5 is not reached and serves as an illustration for if longer polymers or higher concentrations were considered. ESI Figure S2d achieves a similar relaxation time dependence profile as that obtained in previous simulations[5] and experiments.[7]

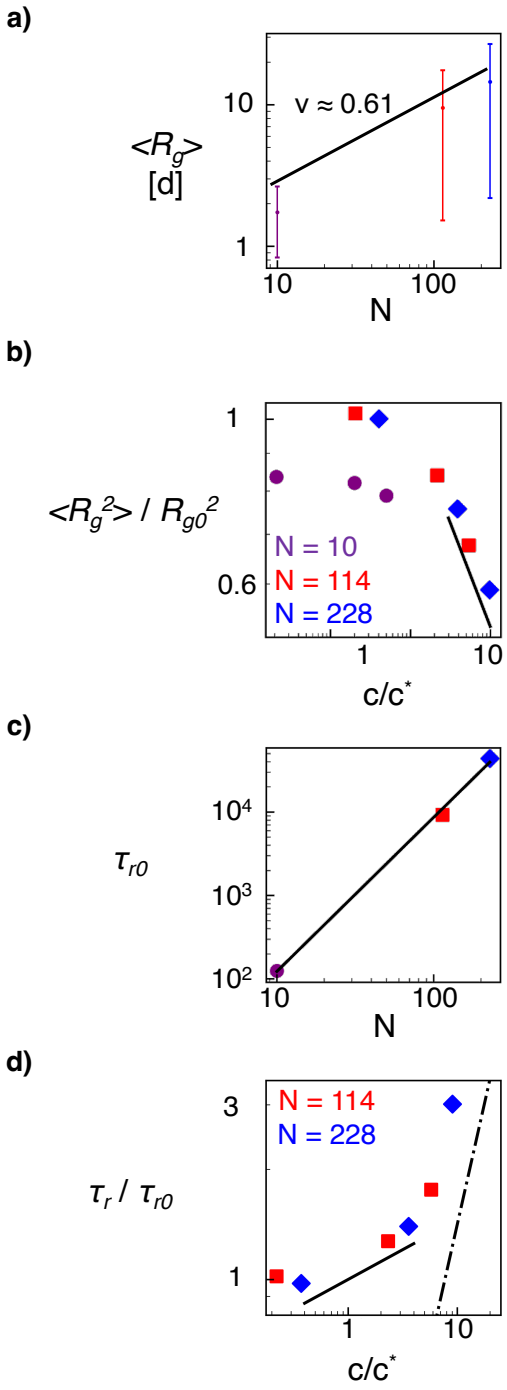

***Figure S3**: Structural and dynamical validation to expected polymer scaling in a good solvent as polymer length N and polymer concentration are varied. a) $\langle R_g \rangle$ scaling for the 1%v dilute systems as N varies. The black line is the scaling prediction from Equation S1 with ν = 0.61. b) relative $\langle R_g^2 \rangle$ scaling as the scaled polymer concentration c/c^* is changed for N = 10 (purple), N = 114 (red,) and N = 228 (blue). The black line is the scaling prediction from Equation S2 with ν = 0.61. c) longest polymer relaxation time at infinite dilution scaling with polymer length. The black line is Equation S3 with ν = 0.615. d) relative longest polymer relaxation time scaling with*

polymer concentration in the semi-dilute regime. The solid black line is the scaling prediction from Equation S4, and the dot-dash black line is the scaling prediction from Equation S5.

We calculate the thermal blob radius using:[2]

$$\xi_T = \frac{b^4}{|v|}$$

with b as the Kuhn segment size. We calculate the excluded volume v by integrating the Mayer f-function using the purely repulsive WCA U(r):[2]

$$v = \int (1 - \exp\left[-\frac{U(r)}{kT}\right] d^3r$$

We find the thermal blob size is ~7.30 d (radius of 3.65 d). For the N = 10 case, the largest R_g (of the least concentrated system 1%v) is 1.74 d, so the polymer length is shorter than the thermal blob size. This is why **Figure S3a** shows the N = 10 system with an R_g^2 below that predicted from scaling relations of a dilute polymer in a good solvent. We further illustrate this point of not following swelling behavior in **Figure S3b** with the N = 10 data lying below the data from N = 114 and 228.

III. Additional information

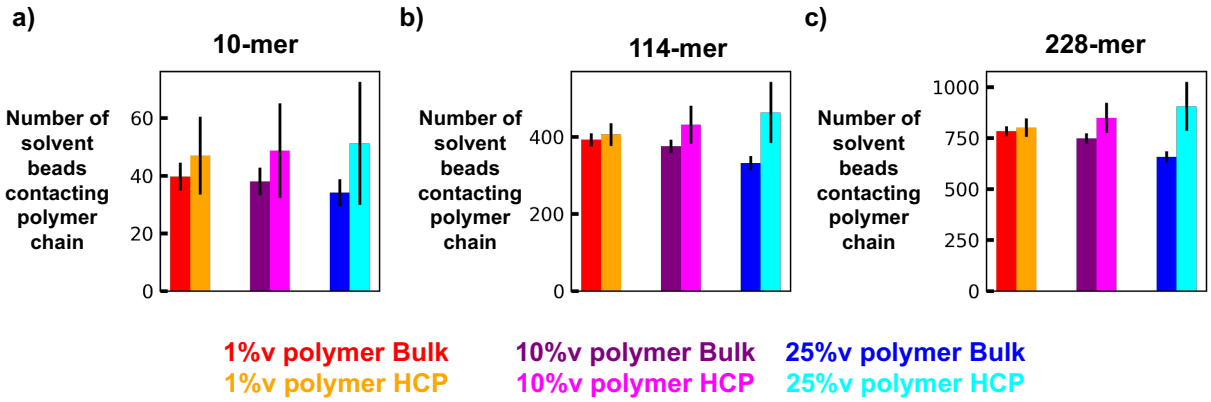

***Figure S4**: Average number of unique solvent beads directly contacting the polymer chain for bulk and HCP confined systems. a), b), and c) display the average number of solvent beads contacting the polymer chain of the N = 10, N = 114, and N = 228 polymer lengths respectively. The red, purple, and blue colors are the bulk polymer results for 1%v, 10%v, and 25%v polymer concentrations. The orange, pink, and cyan colors are the HCP confined polymer results for the 1%v, 10%v, and 25%v polymer concentrations. Error bars are shown as the standard deviation from 3 replicates for all systems except for the N = 228, 1%v, HCP system (orange bar in c)) which is the standard deviation from 10 replicates.*

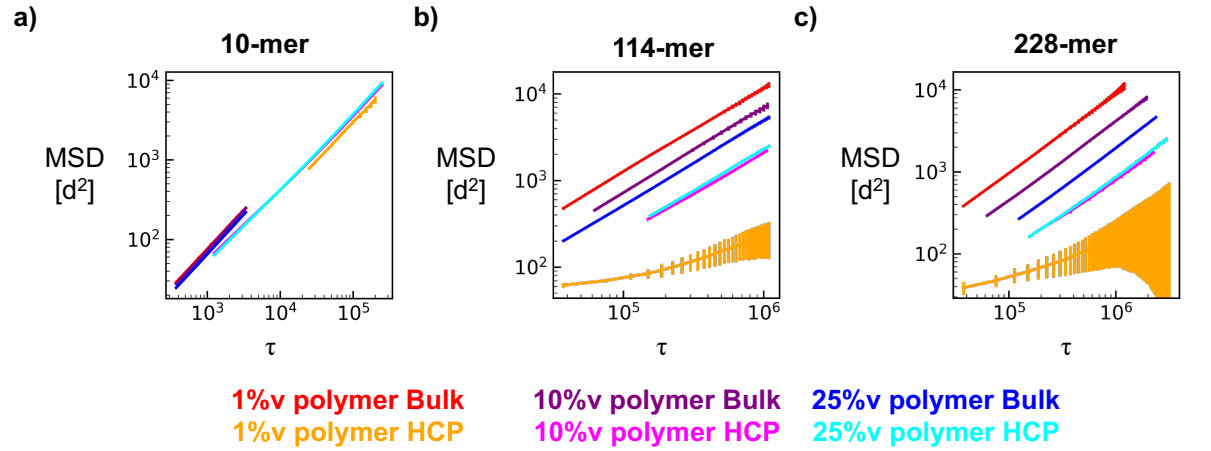

***Figure S5**: Mean squared displacement (MSD) of polymer center of mass for bulk and HCP confined systems. a), b), and c) display the MSD of the N = 10, N = 114, and N = 228 polymer lengths respectively. The red, purple, and blue colors are the bulk polymer results for 1%v, 10%v, and 25%v polymer concentrations. The orange, pink, and cyan colors are the HCP confined polymer results for the 1%v, 10%v, and 25%v polymer concentrations. Error bars are shown as the standard deviation from 3 replicates for all systems except for the N = 228, 1%v, HCP system (orange line in c)) which is from 10 replicates.*

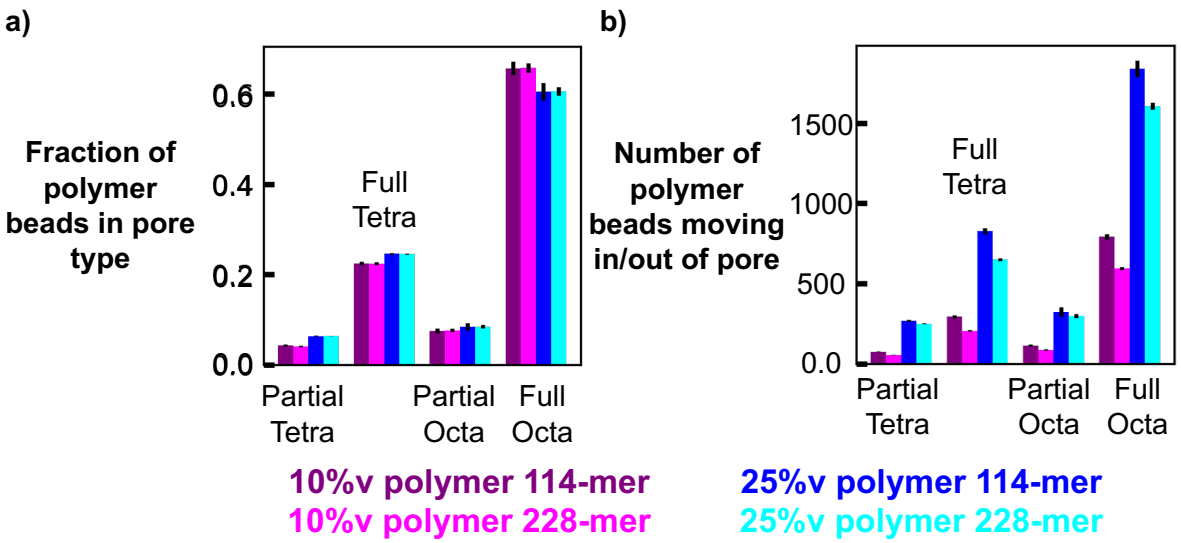

Figure S6*: Determination of polymer localization into nearest tetrahedral or octahedral pore, and the polymer movement between pores broken into the specific pore type. a) describes the fraction of all polymer beads classified as being near to a tetrahedral or octahedral pore broken-down into full pores (pores not interrupted by simulation box edges) and partial pores (pores interrupted by simulation box edges). b) quantifies the number of all polymer beads that either enter or leave a pore over an interval of 156,250 τ. Similar to a), b) categorizes the polymer beads movement between pores for both full pores and partial pores. The error bars for all plots are the standard error of the mean of 3 independent replicates.*

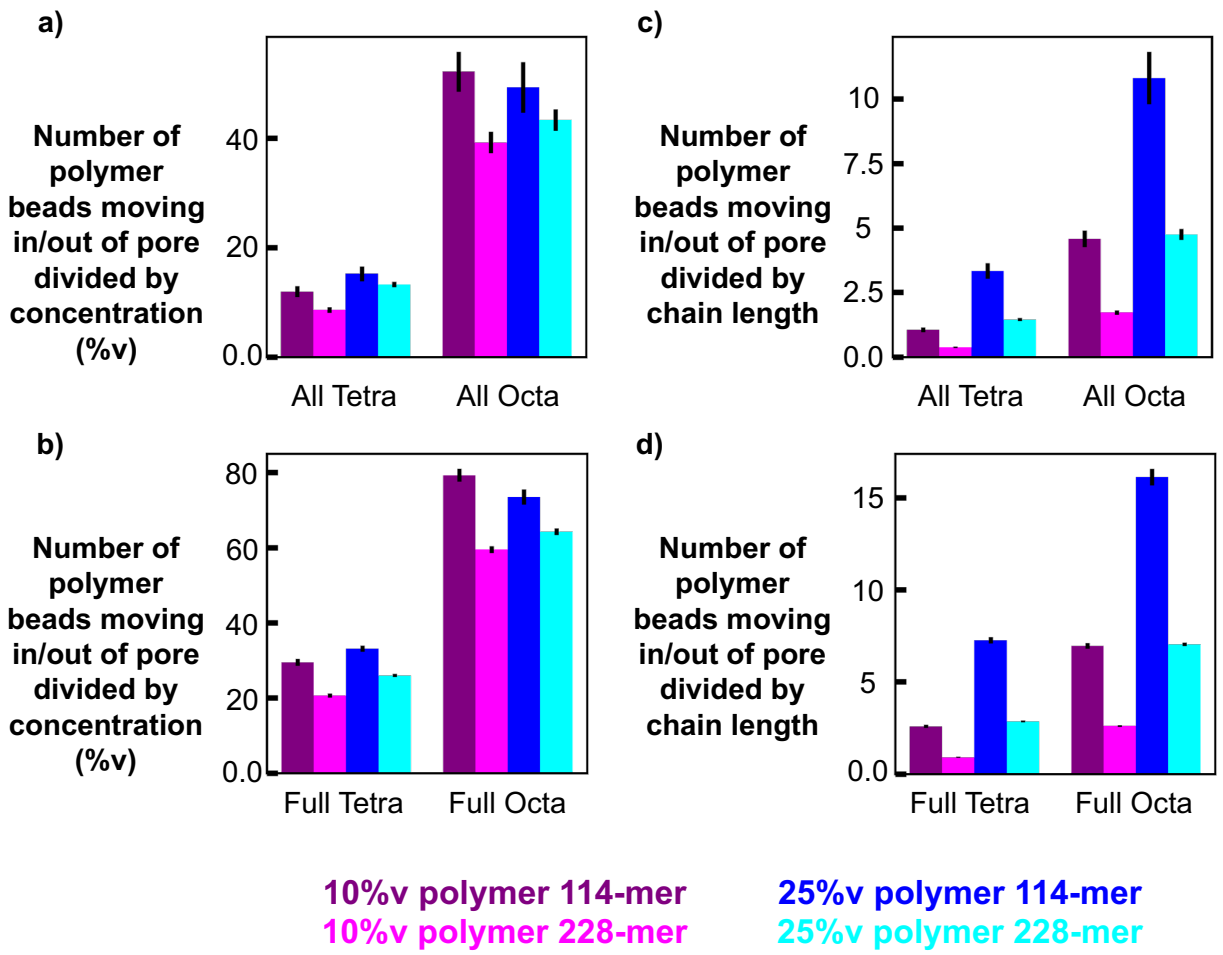

Figure S7*: Determination of polymer movement between tetrahedral and octahedral pores normalized by polymer concentration and polymer chain length. a) and b) quantify the number of all polymer beads divided by the polymer concentration that either enter or leave a pore over an interval of 156,250 τ. b) categorizes the polymer beads movement between pores for only full pores divided by the polymer concentration. c) and d) quantify the number of all polymer beads divided by the polymer chain length that either enter or leave a pore over an interval of 156,250 τ. d) categorizes the polymer beads movement between pores for only full pores divided by the polymer chain length. The error bars for all plots are the standard error of the mean of 3 independent replicates.*

References:

1. L. V. Azaroff, *Introduction to Solids*, McGraw-Hill, 1960.
2. M. Rubinstein and R. H. Colby, *Polymer physics*, Oxford university press New York, 2003.
3. R. H. Colby, *Rheologica acta*, 2010, **49**, 425-442.
4. J. R. Prakash, *Current opinion in colloid & interface science*, 2019, **43**, 63-79.
5. C.-C. Huang, R. G. Winkler, G. Sutmann and G. Gompper, *Macromolecules*, 2010, **43**, 10107-10116.
6. M. Doi, S. F. Edwards and S. F. Edwards, *The theory of polymer dynamics*, oxford university press, 1988.
7. S. S. Patel and K. M. Takahashi, *Macromolecules*, 1992, **25**, 4382-4391.